Pacific Interdecadal Variability in This Century's Sea Surface Temperatures

Yi Chao[1], Michael Ghil[2], Xianjin Li[1], and James C. McWilliams[2]

[1]Jet Propulsion Laboratory, California Institute of Technology
[2]University of California, Los Angeles.

Abstract. Analysis of this century's sea surface temperatures over the Pacific Ocean reveals an interdecadal oscillation with a period of 14–17 years. Our results show that the well-known 1976-77 climate regime shift is not unique, but represents one of several phase transitions associated with this interdecadal oscillation, also found around 1924-25, 1941-42, and 1957-58. The oscillation's striking north-south symmetry across the equator implies strong interactions between tropics and extratropics. A mode with a period of approximately 70 years and an apparently different spatial pattern is also identified tentatively but has to be evaluated further using longer time series.

1. Introduction

The identification of nearly periodic components in natural climate variability can significantly increase the predictability of the Earth's climate system and improve confidence in the detection of anthropogenic climate change. The Pacific Ocean is known to exhibit strong variations on interannual to interdecadal time scales. The interannual fluctuations in the tropical Pacific Ocean are primarily associated with El Niño and the Southern Oscillation (ENSO) phenomenon [Philander, 1990]. Research over the past two decades has resulted in an established theory of ENSO [Neelin et al., 1998] and in predictions of the tropical and extratropical ocean circulation and atmospheric patterns associated with ENSO [Latif et al., 1998].

Recent studies have started to describe Pacific climate variability on time scales longer than interannual [Trenberth and Hurrel, 1994; Zhang et al., 1997]. It has been shown that El Niño and La Niña events have quite different features from one decade to the next [McPhaden, 1999]. Of particular interest are the persistently warm conditions over the tropical Pacific in the early 1990s and their effect on the tropical climate's predictability [Ghil and Jiang, 1998].

Outside the tropics, the North Pacific climate has also undergone several regime shifts during the 20th century, particularly around 1976-77 [Mantua et al., 1997]. The 1976-77 climate regime shift is associated with pronounced changes in the ocean circulation [Deser et al., 1996; Zhang and Levitus, 1997; Zhang et al., 1998; Schneider et al., 1999] that greatly influence the biological productivity [Venrick et al., 1987] and overlying atmosphere [Gershunov and Barnett, 1998]. It is not yet clear, however, to what extent the 1976-77 climate regime shift is unique, and is thus fairly unpredictable, or merely represents the rapid phase transition of an otherwise rather regular, and hence more predictable, oscillatory mode. If the latter is true, what is the characteristic time scale of such an oscillatory mode? What is its spatial pattern: does it encompass the tropics as well as the extratropical North and South Pacific? The possible influence of extratropical Pacific interdecadal variability on the evolution of tropical ENSO is being actively debated [Latif and Barnett, 1994; Gu and Philander, 1996; Kleeman et al., 1999].

We address these questions by analyzing a 92-year (1903–1994) sea surface temperature (SST) time series. Singular spectrum analysis (SSA) is applied to the time series in order to separate and describe oscillatory modes, if present. SSA, which is based on eigenvalue-eigenvector decomposition of a time series' lag-covariance matrix [Dettinger et al., 1995], can decompose a short, noisy time series into a (variable) trend, periodic oscillations, other statistically significant (but aperiodic) components, and noise. When two eigenvalues are nearly equal and the corresponding Principal Components (PCs) are in phase quadrature, they capture a (nonlinear) oscillation. Spatial patterns associated with climate regime shifts will be related to the phase evolution of these oscillatory modes.

2. Sea Surface Temperature Dataset

The Global Ice Sea Surface Temperature (GISST) data set [Jones, 1994; Parker et al., 1995] is used in the present study. The challenge of working with a century-long SST time series is the poor spatial coverage, particularly before 1950s. Analysis of global averaged SST [Ghil and Vautard, 1991; Plaut et al., 1995] does not discriminate among signals from individual basins. To isolate basin-specific spatio-temporal patterns associated with low-frequency modes requires the use of multivariate signals [Mann and Park, 1994; Moron et al., 1998]. In order to avoid the sampling problem for the latter, we analyze a SST persistence index rather than the SSTs themselves. The SST persistence index is measured by lagged spatial correlations, which have been used in both atmospheric [Mo and Ghil, 1987] and oceanographic [Namias et al., 1988] analyses of regime shifts and their predictions. The lagged spatial correlation $R(t, \tau)$ at time t with respect to the time lag τ is defined by:

$$R(t,\tau) = \frac{\sum_x \sum_y \left(T(x,y,t) - \overline{T(x,y,t)}\right)\left(T(x,y,t+\tau) - \overline{T(x,y,t+\tau)}\right)}{\sqrt{\sum_x \sum_y \left(T(x,y,t) - \overline{T(x,y,t)}\right)^2 \sum_x \sum_y \left(T(x,y,t+\tau) - \overline{T(x,y,t+\tau)}\right)^2}}\ ; \qquad (1)$$

here $T(x, y, t)$ is the SST anomaly at location (x, y) and time t, $\sum_x \sum_y$ represents the double sum with respect to (x, y), and the overbar represents the mean anomaly averaged over the domain.

The original GISST dataset consists of monthly values on a 1° x 1° grid. The climatological annual cycle is obtained by averaging for each calendar month over the 92 years and removed from the monthly time series. The resulting monthly SST anomalies are used in calculating the SST persistence index as an average of lagged pattern correlations:

$$S(t) = \sum_\tau R(t, \tau)/12, \qquad (2)$$

where $\sum_\tau$ represents the sum over time lags from 1 to 12 months. The domain for this calculation is the North Pacific (20°N–60°N; 140°E–120°W). Qualitatively the same results are obtained when the domain includes the tropical and even the South Pacific.

3. Results

Figure 1 (dotted line) shows the monthly values of the SST persistence index $S(t)$ with a 2-year running mean applied. Interannual fluctuations clearly dominate the extratropical North Pacific's variability, consistent with the recent analysis of Zhang et al. [1998]. However, lower-frequency variability in the persistence is also apparent, with a sharp increase around the middle of the century. To isolate the lower-frequency features, we apply SSA as a nonparametric low-pass filter with a window width of 500 months. The two leading PCs describe 38.2% of the total variance, and are clearly separated from the remaining PCs, all of which lie below 7% of variance. Projection of the time series onto these two leading modes is shown as the solid line in

Fig. 1. From the first to the second half of the century, the North Pacific's persistence almost doubles: from 0.15 during the 1920s and 1930s to 0.30 during the 1960s and 1970s.

This increase of SST persistence is associated with a coherent spatial structure. Figure 2 shows the difference map of SST anomalies subtracting the low-persistence phase (1920–1940) from the high-persistence phase (1955–1975), marked by the "L" and "H" signs in Fig. 1, respectively. Most parts of the North Pacific Ocean warm from the first to the second half of the 20th century, with an amplitude that exceeds 0.4°C. A somewhat smaller warming of 0.2°C is seen in the western South Pacific, and a 0.2°C cooling is seen in the eastern equatorial and South Pacific. The small areas of largest warming and cooling near the Pacific's northern and southern boundaries and off Japan may be genuine oceanographic signals or due to the poor spatial sampling. Examination of the global patterns (see Fig. 3 of Moron et al. [1998]) indicates that this North Pacific warming exceeds considerably the global warming trend during 1920–1970. Based on this single realization of an alternation between low and high persistence, its near-periodicity is estimated to be around 70 years, close to that suggested by global temperatures [Schlesinger and Ramankutty, 1994] and climate proxy records [Mann et al., 1998].

The residual time series (dotted line in Fig. 3) is obtained by subtracting the SSA-reconstructed centennial mode above from the original time series. In order to separate interdecadal variability from interannual variations, SSA is again applied to the residual time series with a smaller window width of 240 months; the results so obtained have greater statistical significance. The two leading PCs form a pair which describes 28.8% of the residual variance, and are clearly separated from the other PCs (not shown); this pair is thus deterministic and oscillatory, rather than stochastic. Our spectral analysis on the SSA-reconstructed time series (solid line in Fig. 3) based on the two leading PCs reveals a spectral peak with a period of 14–17 years (not shown). On the interdecadal time scale, the SST persistence index over the North Pacific varies with a range of 0.1. With respect to the mean persistence of 0.25 (see Fig. 1), Pacific SSTs during one decade could be more (or less) persistent than the next decade by almost 40%.

Swings of our index from high to low persistence or vice-versa correspond to coherent basin-wide patterns. Figure 4 shows SST difference maps between two consecutive 5-year means separated by two years each, i.e., subtracting the high-persistence phase (earlier interval) from the low-persistence phase (later interval) marked by "H" and "L" in Fig. 3, respectively. The first and last transitions are not presented because of the insufficient data at either end of the time series. The transition around 1941-42 is excluded because it nearly coincides with the centennial mode's transition (see Fig. 1), which has comparable amplitude (see Fig. 2).

Among the three phase transitions centered at 1924-25, 1957-58, and 1976-77, the interdecadal regime shift around 1976-77 (Fig. 4c) is clearly the strongest, with a peak-to-peak amplitude that exceeds 0.8°C. The transitions around 1924-25 and 1957-58 (Figs. 4a, b) are more modest, but still have a peak-to-peak amplitude on the order of 0.4°C. The characteristic spatial pattern associated with the three transitions around 1924-25, 1957-58, and 1976-77 is robust: cooling occurs in the western and central North and South Pacific, while warming is seen in the eastern equatorial Pacific and also along the coasts of North and South America. In all three cases, there is an approximate north-south symmetry across the equator, slightly distorted by the shape of the basin.

4. Summary

Analyzing this century's Pacific SSTs, we conclude that the 1976-77 climate regime shift is not unique, but represents the single largest phase transition of a nearly periodic interdecadal oscillation. Similar climate regime transitions are also found around 1957-58, 1941-42, and 1924-25. We conducted several independent tests to confirm our findings with the SSA analysis. We compared the SSA-reconstructed interdecadal time series with the 6-year running mean of the residual time series. The time series shows slightly more temporal irregularity than the fomer, but the correlation between the two is 0.79. The regime transitions around 1957-58 and 1976-77 have also been confirmed by an independent, 49-year (1945–93) time series derived from the Comprehensive Ocean-Atmosphere Data Sets [Da Silva et al., 1994].

The spatial structure associated with this Pacific interdecadal mode is roughly north-south symmetric across the equator. Previous studies have discussed spatial patterns of broad-band interdecadal variability in the North and eastern equatorial Pacific; this broad-band variability's signature in the South Pacific and its north-south symmetry across the equator have only been pointed out quite recently [White and Cayan, 1998]. The present results are substantially sharper in that they capture the Pacific basin-wide interdecadal variability's near periodicity and associate it clearly with a repetition of fairly abrupt regime transitions. The cross-equatorial symmetry of this well-defined mode of variability strongly suggests that it involves both tropical and extratropical processes. The specific pathways linking the tropical and extratropical signals are currently under intense study. The spatio-temporal evolution described in this study provides the needed information to test the existing hypotheses and to verify numerical models of Pacific interdecadal variability.

The centennial mode we have identified as changing the phase of SST persistence around the middle of the 20th century coincides with a warming of up to 0.5°C of the North Pacific from the century's first to its second half. Because the length of the time series covers only one realization of this centennial mode, it must be considered as provisional and subject to revision when longer time series become available. Further understanding and successful simulation of these Pacific low-frequency modes are crucial to predict their meteorological and biological consequences and to distinguish them from anthropogenic climate change.

Acknowledgments. This work was performed, in part, at the Jet Propulsion Laboratory (JPL), California Institute of Technology under contract with the National Aeronautics and Space Administration (NASA). MG's work was supported by NASA Grant NAG5-713 and a National Science Foundation (NSF) Special Creativity Award. JCM was supported by NSF Grant OCE-9633681. The use of the GISST data (obtained from JPL Physical Oceanography-Distributed Active Archive Center) and the SSA-MTM Toolkit (http://www.atmos.ucla.edu/tcd/) are gratefully acknowledged.

References

Da Silva, A.M., C.C. Young, and S. Levitus, Atlas of surface marine data 1994, Vol. 1: Algorithms and procedures, NOAA Atlas NESDIS, US Dept. Of Commerce, 83pp, 1994.

Deser, C., M.A. Alexander, M.S. Timlin, Upper-ocean thermal variations in the North Pacific during 1970-1991, *J. Climate, 9,* 1840, 1996.

Dettinger, D., M. Ghil, C.M. Strong, W. Weibel, and P. Yiou, Software expedites singular spectrum analysis of noisy time series, *Eos, Trans. Amer. Geophys. Union, 76,* 12, 1995.

Ghil, M., and R. Vautard, Interdecadal oscillations and the warming trend in global temperature time series, *Nature, 350,* 324, 1991.

Gershunov, A., and T.P. Barnett, Interdecadal modulation of ENSO teleconnection, *Bull. Am. Meteorol. Soc., 79*, 2715, 1998.

Ghil, M., and N. Jiang, Recent forecast skill for the El Niño/Southern Oscillation. Geophys. Res. Lett., 25, 171, 1998.

Gu, D., and S.G.H. Philander, Interdecadal climate fluctuations that depend on exchanges between the tropics and extratropics, *Science, 275,* 805, 1996.

Jones, P.D., Hemispheric surface air temperature variations: A reanalysis and an update to 1993, *J. Climate, 7*, 1794, 1994.

Kleeman, R., J.P. McCreary, Jr., B.A. Klinger, A mechanism for generating ENSO decadal variability, *Geophys. Res. Lett., 26,* 1743, 1999.

Latif, M., and T.P. Barnett, Causes of decadal climate variability over the North Pacific and North America, *Science, 266*, 634, 1994.

Latif, M., D. Anderson, T. Barnett, M. Cane, R. Kleeman, A. Leetmaa, J. O'Brien, A. Rosati, and E. Schneider, A review of the predictability and prediction of ENSO, *J. Geophys. Res., 103*, 14375, 1998.

Mann, M.E., and J. Park, Global-scale modes of surface-temperature variability on interannual to century time scales, *J. Geophys. Res., 99,* 25819, 1994.

Mann, M.E., R. S. Bradley, M. K. Hughes, Global-scale temperature patterns and climate forcing over the past six centuries, *Nature, 392*, 779, 1998.

Mantua, N.J., S.R. Hare, Y. Zhang, J.M. Wallace, and R.C. Francis, A Pacific interdecadal climate oscillation with impacts on salmon production, *Bull. Am. Meterol. Soc., 78*, 1069, 1997.

McPhaden, M.J., Genesis and evolution of the 1997-98 El Niño, *Science, 283*, 950, 1999.

Mo, K., and M. Ghil, Statistics and dynamics of persistence anomalies, *J. Atmos. Sci., 44*, 877, 1987.

Moron, V., R. Vautard, M. Ghil, Trends, interdecadal and interannual oscillations in global sea surface temperatures, *Clim. Dyn., 14,* 545, 1998.

Namias, J., X. Yuan, D. R. Cayan, Persistence of North Pacific sea surface temperature and atmospheric flow patterns, *J. Climate, 1*, 682, 1988.

Neelin, D.J., D.S Battisti, A.C. Hirst, F.-F. Jin, Y. Wakata, T. Yamagata, and S.E. Zebiak, ENSO theory, *J. Geophys. Res., 103*, 14261, 1998.

Parker, C.K., C.K. Folland, M. Jackson, Marine surface temperature: observed variations and data requirements, *Climate Change, 31*, 559, 1995.

Philander, S.G.H., *El Niño, La Niña and the Southern Oscillation*, Academic Press, New York, 1990.

Plaut, G., M. Ghil, R. Vautard, Interannual and interdecadal variability in 335 years of central England temperatures, *Science, 268*, 710, 1995.

Schlesinger, M.E., and N. Ramankutty, An oscillation in the global climate system of period 65-70 years, *Nature, 367*, 723, 1994.

Schneider, N., A.J. Miller, M.A. Alexander, C. Deser, Subduction of decadal North Pacific temperature anomalies: observations and dynamics, *J. Phys. Oceanogr., 29,* 1056, 1999.

Trenberth, K., and J.W. Hurrel, Decadal atmosphere-ocean variations in the Pacific, *Climate Dyn., 9,* 303, 1994.

Venrick, E.L., J.A. McGowan, D.R. Cayan, T.L. Hayward, Climate and Chlorophyll a: Long-term trends in the central North Pacific Ocean, *Science, 238*, 70, 1987.

White, W.B., and D. R. Cayan, Quasi-periodicity and global symmetries in interdecadal upper ocean temperature variability, *J. Geophys. Res., 103*, 21335, 1998.

Zhang, Y., J.M. Wallace, D. Battisti, ENSO-like interdecadal variability: 1900–93, *J. Climate, 10,*

1004, 1997.

Zhang, R.-H., and S. Levitus, Structure and cycle of decadal variability of upper-ocean temperature in the North Pacific, *J. Climate, 10,* 710, 1997.

Zhang, R.-H., L.M. Rothstein, A.J. Busalacchi, Origin of upper-ocean warming and El Niño changes on decadal scales in the tropical Pacific Ocean, *Nature, 391*, 879, 1998.

Zhang, X., J. Sheng, A. Shabbar, Modes of interannual and interdecadal variability of Pacific SST, *J. Climate, 11*, 2556, 1998.

Yi Chao and Xianjin Li, Jet Propulsion Laboratory, 4800 Oak Grove Drive, Pasadena, CA 91109 (e-mail: Yi.Chao@jpl.nasa.gov, xjl@pacific.jpl.nasa.gov)

Michael Ghil and James C. McWilliams, University of California, Los Angeles, 405 Hilgard Avenue, Los Angeles, CA 90095 (e-mail: ghil@atmos.ucla.edu, jcm@atmos.ucla.edu)

(submitted December xx, 1999)

Figure Captions

Figure 1. The original time series (dotted line) of the SST persistence index during 1903–1994 and SSA reconstruction based on the two leading PCs (solid line).

Figure 2. The SST difference map between two 20-year means, separated by fifteen years, subtracting the earlier time interval (1920–1940) from the latter one (1955–1975). The contour interval is 0.2 °C.

Figure 3. The residual time series (dotted line) and the reconstruction (solid line) based on the two leading PCs of a second SSA analysis.

Figure 4. SST difference maps between two 5-year means, separated by two years each, with the earlier interval subtracted from the latter one: (a) 1919–1923 and 1926–1930, (b) 1952–1956 and 1959–1963, and (c) 1971–1975 and 1978–1982. The contour interval is 0.2 °C.

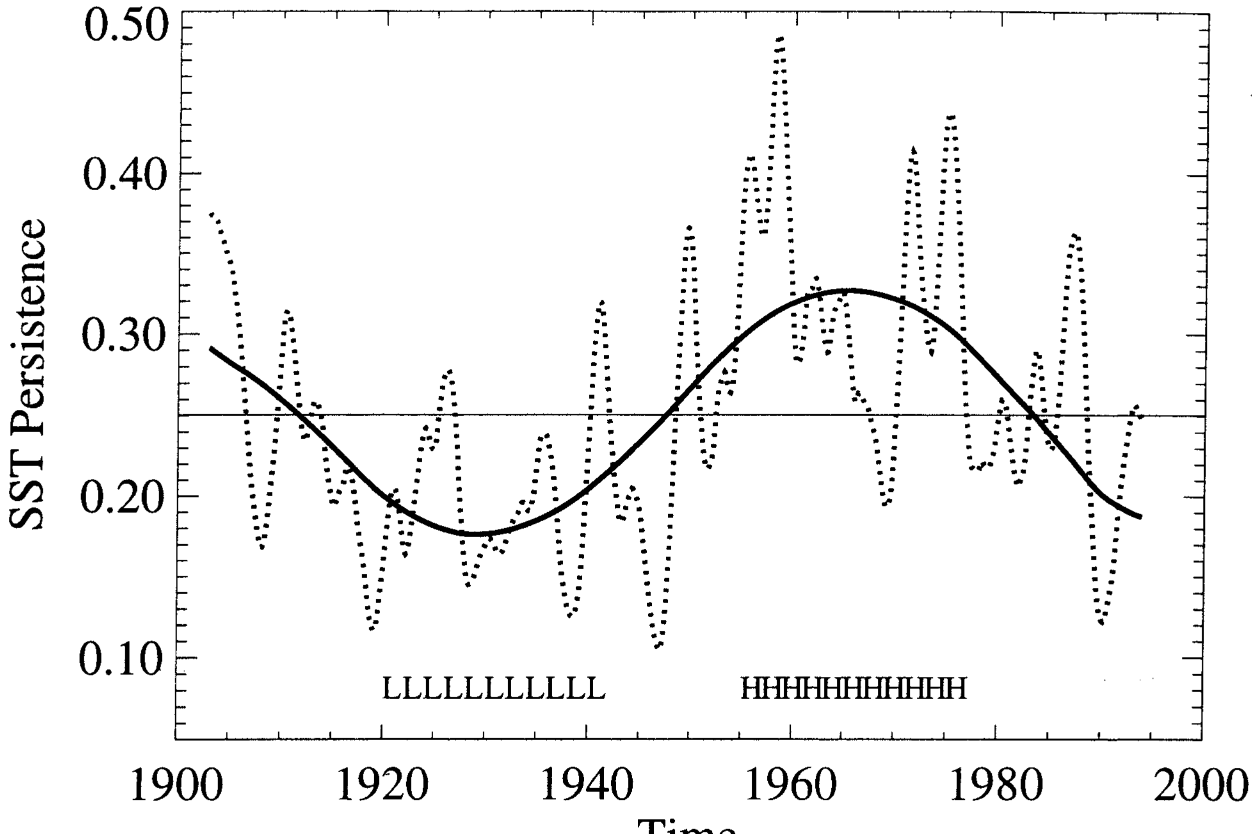

Figure 1

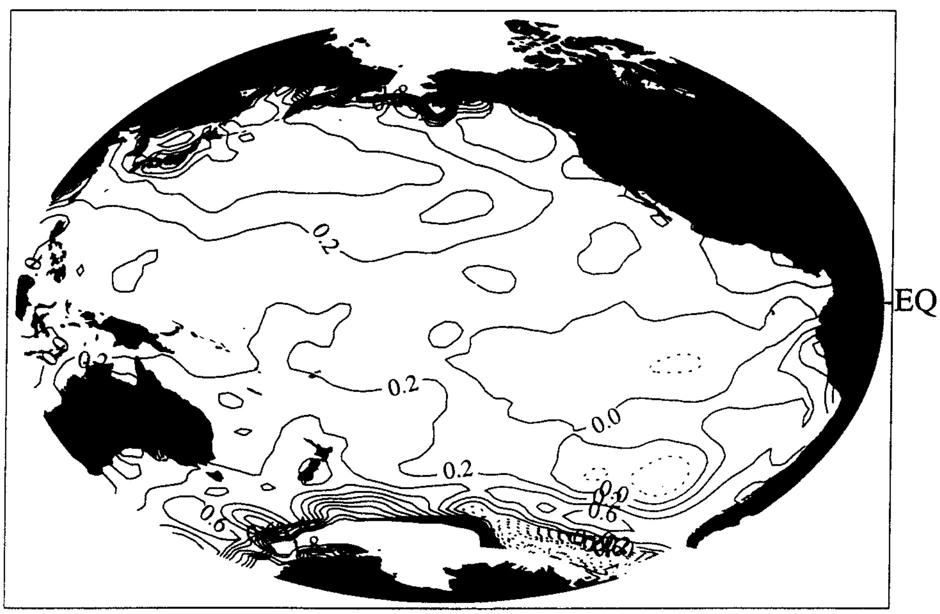

Figure 2

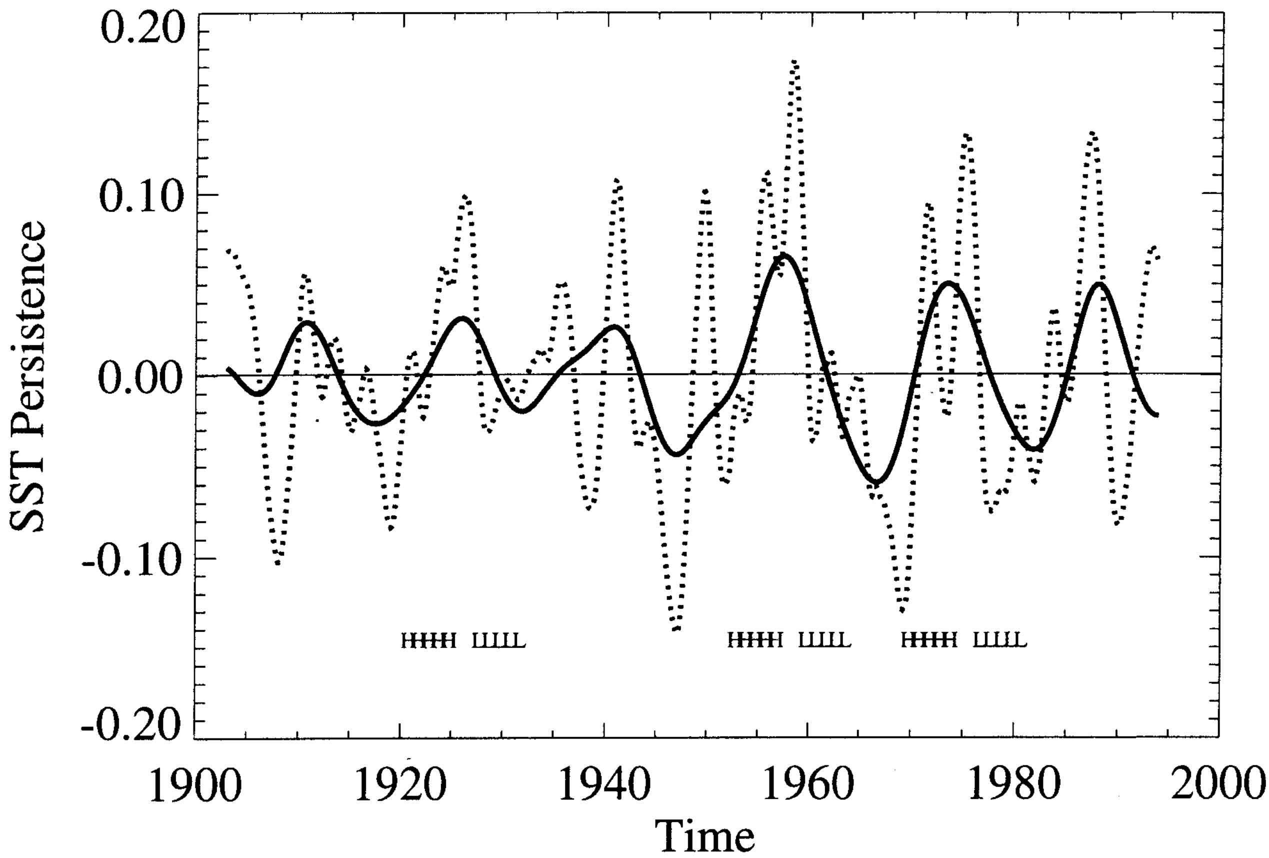
0.20
0.10
0.00
-0.10
-0.20
SST Persistence
HHHH LLLL
HHHH LLLL
HHHH LLLL
1900
1920
1940
1960
1980
2000
Time

Figure 3

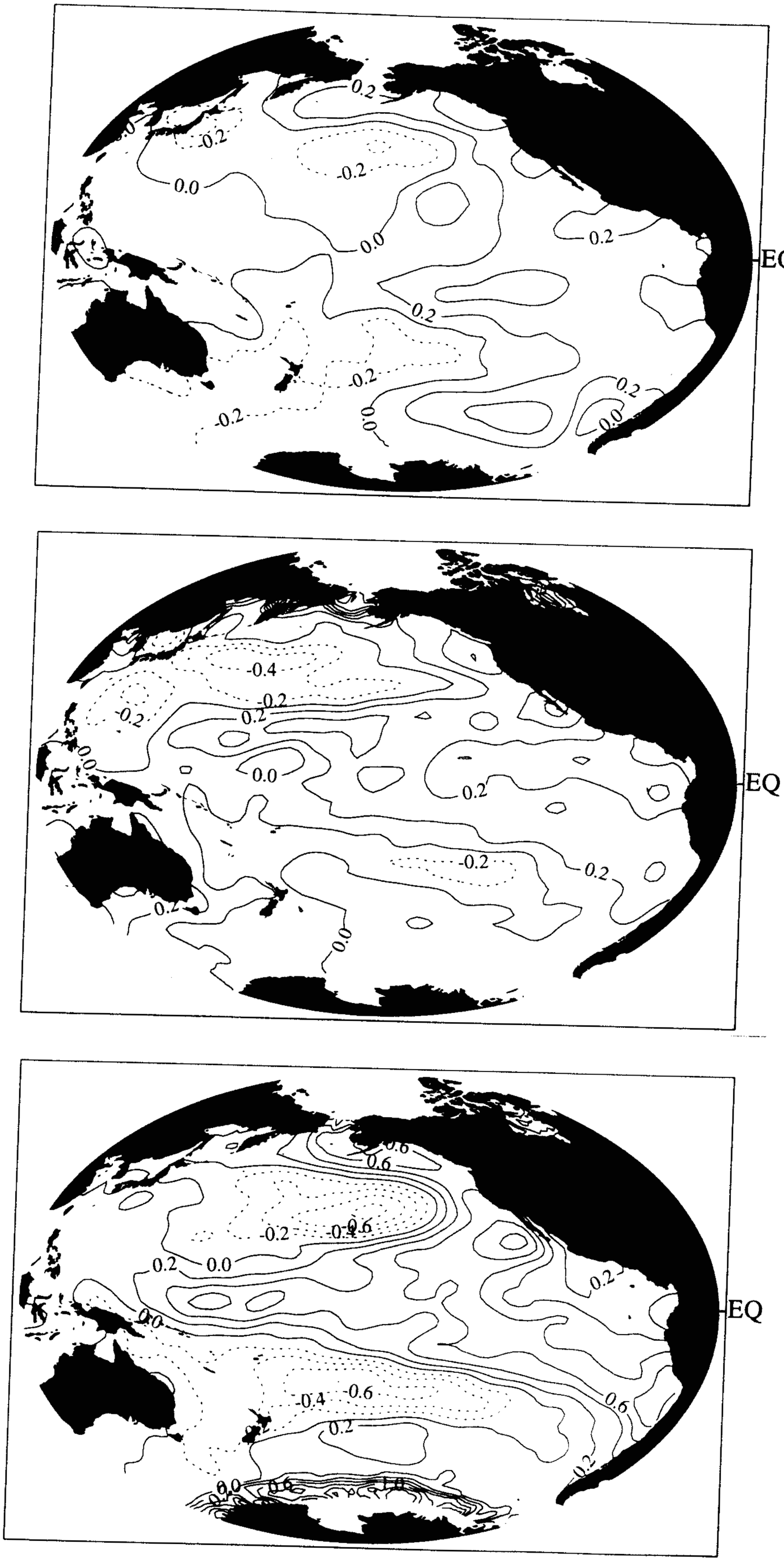

0.2
-0.2
-0.2
0.0
0.0
0.2
EQ
0.2
-0.2
0.0
0.2
0.0
-0.2
-0.4
-0.2
0.2
-0.2
0.0
0.0
0.2
EQ
-0.2
0.2
0.2
0.0
0.6
0.6
-0.2
-0.4
0.6
0.2
0.0
0.2
0.0
EQ
-0.4
-0.6
0.6
0.2
0.2
0.0
0.6
1.0

(a)

(b)

(c)

Figure 4